ACS OMEGA

Open Access

http://pubs.acs.org/journal/acsodf

Article

Oxidized Cellulose Nanocrystals from Durian Peel Waste by Ammonium Persulfate Oxidation

Henny Pratiwi, Kusmono,* and Muhammad Waziz Wildan

Cite This: *ACS Omega* 2023, 8, 30262−30272

Read Online

ACCESS | Metrics & More | Article Recommendations

ABSTRACT: Cellulose nanocrystals (CNCs) have gained much attention due to their biodegradable, renewable, nontoxic, and inexpensive nanomaterials with some remarkable properties. In this study, cellulose nanocrystals from durian peel waste were isolated by chemical oxidation. This process involved two stages of a chemical process, namely, bleaching followed by oxidation of ammonium persulfate (APS). The impact of process parameters (APS concentrations and oxidation temperatures) on the oxidized CNC was assessed. The properties of CNC were investigated by attenuated total reflection-infrared (ATR-IR) spectroscopy, X-ray diffraction (XRD), thermogravimetric analysis (TGA), and transmission electron microscopy (TEM). ATR-IR results showed that the structure of cellulose did not change during APS oxidation. XRD results indicated that APS oxidation improved the crystallinity index by 103% due to the removal of the amorphous components. The resulting CNC was needlelike in shape and had an average width range of 5.00−7.81 nm, a length range of 114.52−126.83 nm, and an aspect ratio range of 16.76−24.20. From the TGA analysis, the thermal stability was found to increase with increasing oxidation temperature. The optimum conditions for a maximum crystallinity index and the highest thermal stability were obtained at 80°C oxidation with 1 M APS. Therefore, APS oxidation was a remarkable method for increasing the value of durian peel waste into high-value nanocellulose.

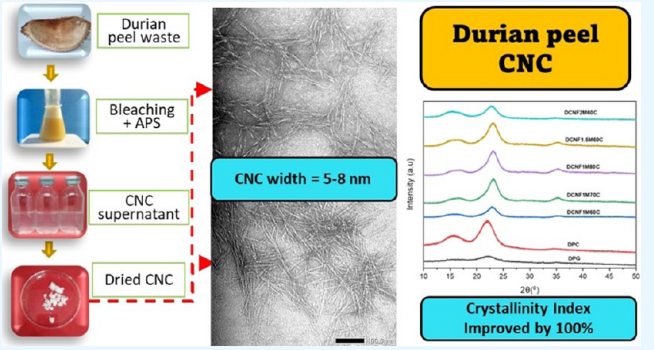

1. INTRODUCTION

Nanocellulose is a cellulose material with nanoscale structural dimensions of a certain size. The three types of nanocellulose, called cellulose nanofibers (CNFs), cellulose nanocrystals (CNCs), and bacterial nanocellulose, are known for their excellent properties, such as nontoxicity, biodegradability, and biocompatibility with minimal effects on health and the environment compared to the synthetic one. In addition, its other advantages, including a high aspect ratio, a low thermal expansion coefficient, a high tensile strength, and favorable optical characteristics, make it suitable for use in a variety of applications, including the production of paper, optically transparent films, coating agents, stretchable sensors, energy harvesting devices, and applications for lightweight materials like ballistic protection. Nanocellulose also has the potential to be applied in the biopharmaceutical field, such as in drug delivery systems and temporary implants.[1−4]

The extraction and production of nanoscale cellulose have been widely discussed by researchers in recent years. However, its application as a reinforcing agent to produce composites in novel applications is a relatively recent study and has attracted increasing interest among nanotechnology researchers. This is because compared to cellulose, the nanocellulose material is lighter, has higher stiffness and strength, and has a high surface area-to-volume ratio.[5] Moreover, nanocellulose can act as a strengthening agent to develop environmentally friendly bionanocomposites for various types of industrial applications.[6] One of the challenges in producing biocomposites is the hydrophilic nature of the materials in most natural sources. This property will result in poor interfacial bonding when combined with hydrophobic polymers. Therefore, it is important to modify the surface of the CNC so that it has good interfacial properties with the hydrophobic polymer matrix.

Several methods have been carried out to produce CNCs from natural materials, such as mechanical, chemical, and a combination of mechanical and chemical techniques.[7−11] Ammonium persulfate (APS) is one of the chemical treatments using the oxidation method used to isolate CNCs from natural products. During the isolation process, some surface hydroxyl

Received: May 5, 2023
Accepted: July 31, 2023
Published: August 11, 2023

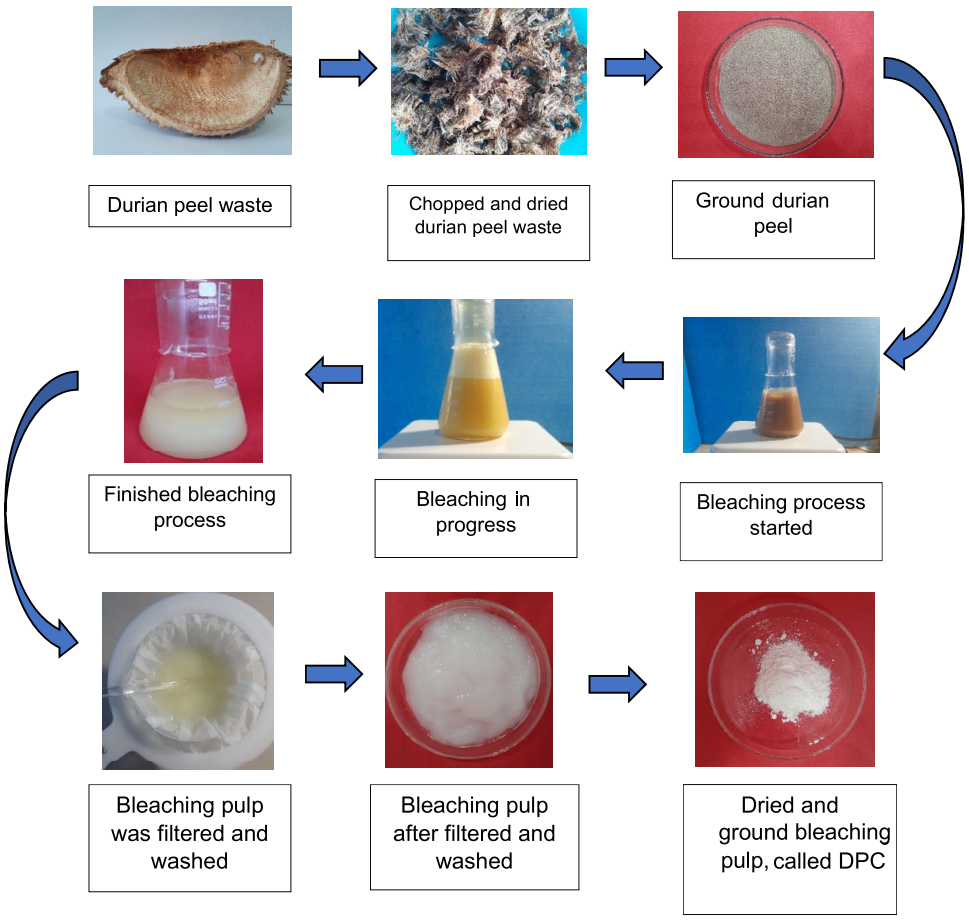

Figure 1. Preparation of durian peel cellulose.

groups were oxidized, resulting in carboxyl groups of CNCs.[6,12,13] Therefore, some of the hydroxyl (OH) groups are substituted with carboxyl (COOH) groups during the APS oxidation process. Replacing some of the hydroxyl groups present in CNCs with carboxyl groups results in a decrease in the hydrophilic nature of the CNC. This means that the hydrophobic properties of the CNC increase, so that it can increase the interaction between CNC particles and the polymer matrix, especially hydrophobic ones such as polyester. Some of the advantages of APS compared to other methods are low cost, low long-term toxicity, and better thermal stability when contrasted with conventional hydrolysis using sulfuric acid.[14,15]

With APS oxidation, it is possible to extract nanocellulose more easily than with other procedures, with less pollution produced than acid hydrolysis and less energy used than mechanical treatment.[16] Surface treatment with APS oxidation has been proven effective and successful in producing nanocellulose by removing lignin, hemicellulose, and other amorphous contents.[17] Many factors affect the characteristics of CNCs during the APS oxidation process such as the source of cellulose, the APS concentration, oxidation temperature, and reaction time. Until now, many researchers have studied the characteristics and performance of various types of nanocellulose by APS oxidation.[7,14−16,18−22]

Lemon seeds have been successfully used by Zhang et al. to extract nanocrystalline cellulose using two different methods, i.e., oxidation and acid hydrolysis.[15] Two oxidation methods were used in this study: TEMPO oxidation and APS oxidation. In contrast, nanocellulose resulting from TEMPO oxidation has a higher yield, larger CNC size, and lower crystal index when compared with nanocellulose resulting from APS oxidation and acid hydrolysis. However, APS oxidation produced CNCs with the highest crystal index. A comparison of nanocellulose isolation methods was also investigated by Yang et al., where the raw material used was *Miscanthus x. giganteus*. The results were almost the same, where APS oxidation resulted in a higher crystallinity index than TEMPO oxidation and better thermal stability than acid hydrolysis.[22]

The durian tree is one of the plants that can thrive in Indonesia and has even become the king of fruit trees. So far, the presence of durian peel as organic waste is abundant and its utilization is still not optimal. Some examples of utilizing durian peel waste include raw materials for briquettes, vegetable pesticides, and antibacterial agents.[23−25] Another research[26] reported that durian peel contains high cellulose (around 68.1%), so it has great potential to be used as a source of cellulose in the manufacture of CNCs which can then be used as a composite reinforcement material. Compared to other sources of cellulose, such as bamboo, wood, and grass, durian peel, which is abundantly available in Indonesia, has several advantages like higher cellulose content, but it still has limited utilization. As far as the research is concerned, investigations into the manufacture of CNCs sourced from durian peels using the APS oxidation method have not been reported by other researchers. Therefore, it is interesting to study the manufacture of CNCs from durian peel waste using the APS oxidation method. In this study, the effects of isolation

https://doi.org/10.1021/acsomega.3c03117
ACS Omega 2023, 8, 30262−30272

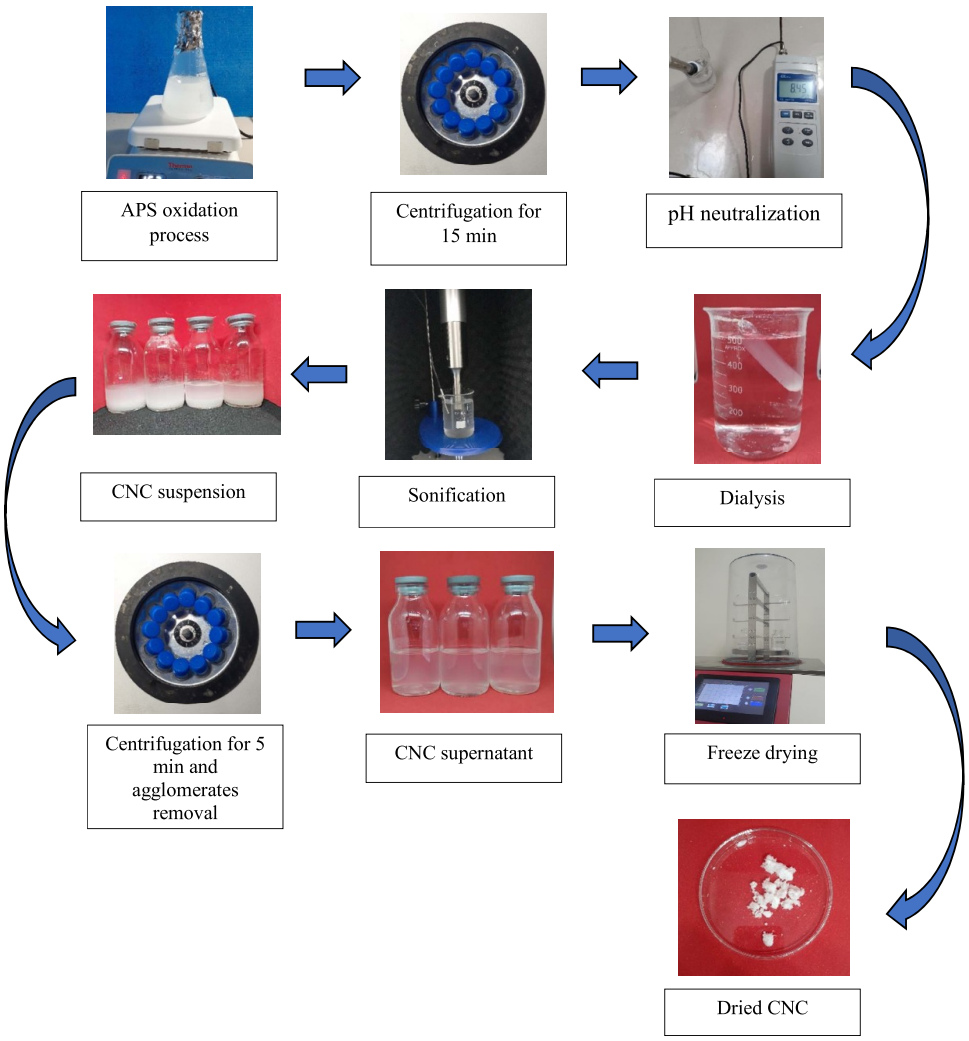

Figure 2. Preparation of CNCs by APS oxidation.

parameters, precisely the oxidation temperature and APS concentration, on the characteristics of CNCs were examined. Optimal oxidation parameters were expected to be obtained from this work so that the produced CNCs can be used effectively as reinforcement in biocomposites.

2. EXPERIMENTAL SECTION

2.1. Materials. Durian peel waste was obtained from durian fruit grown in the Kulon Progo Regency, Yogyakarta Special Province, Indonesia. Sodium chlorite (25%), glacial acetic acid for analysis, sodium hydroxide (NaOH) for analysis, and ammonium persulfate (APS) were purchased from Merck Ltd.

2.2. Pretreatment of Durian Peel Waste. The durian peel cellulose (DPC) was isolated according to a method done by another researcher with slight modifications.[22] Durian peel waste was taken for the whole center (including spines, locules, and white skin spaces), with a distance of a quarter from the stalk and a quarter from the shoot. Durian peel was cleaned thoroughly with running water and dried under the sun for 7 days or until dry. Furthermore, the durian peel was pulverized to pass an 80 mesh sieve to obtain a durian peel ground (DPG). Subsequently, distilled water, 0.5 mL of acetic acid, and 8 wt % sodium chlorite were mixed so that the volume of the solution became 80 mL. The mixture of the solution and durian peel powder (4 g) was then heated while continuously stirring with a magnetic stirrer at 70 °C for 2 h. This process is called the bleaching process. After being filtered (resulting in bleaching pulp) and washed repeatedly with distilled water, the resulting residue was oven-dried at 60 °C and ground to produce durian peel cellulose (DPC) powder. The yield of DPC by the above bleaching pretreatment process was almost 2 g (50%). The hemicellulose and lignin contents of DPC after bleaching were 21.98 and 9.06%, respectively. The preparation of durian peel cellulose is illustrated in Figure 1.

2.3. Isolation of Cellulose Nanocrystals. After pretreatment, CNC isolation was carried out through an oxidation process using APS. DPC powder was blended with the APS solution (1, 1.5, and 2 M concentrations), and the mixture was agitated for 16 h at varied temperatures of 60, 70, and 80 °C. When the solution reached room temperature, the suspension was centrifuged 3 times, and distilled water was added to wash the CNC to reduce the acidity of the suspension. The suspension was neutralized by 1 M NaOH addition until the pH reached 7. Afterward, the suspension was dialyzed with distilled water for 5 days, and the concentration of the suspension was 0.1%. Centrifugation was carried out to separate the supernatant and precipitate for 5 min. The large particles were then removed, and the supernatant was sonicated for 2 min by using an ultrasonic homogenizer (20 kHz, 200 W) and lyophilized to obtain durian cellulose

https://doi.org/10.1021/acsomega.3c03117
ACS Omega 2023, 8, 30262−30272

Table 1. Oxidation Parameters and CNC Yields

samples	process conditions	APS concentration (M)	oxidation temperature (°C)	yield (%)
DPG	raw durian peel, ground	-	-	-
DPC	durian peel after bleaching pretreatment	-	-	50
DCNC1M70C		1	70	32.26
DCNC1M60C		1	60	30.11
DCNC1M80C	combination of bleaching pretreatment and APS oxidation	1	80	35.67
DCNC1.5M60C		1.5	60	24.79
DCNC2M60C		2	60	17.65

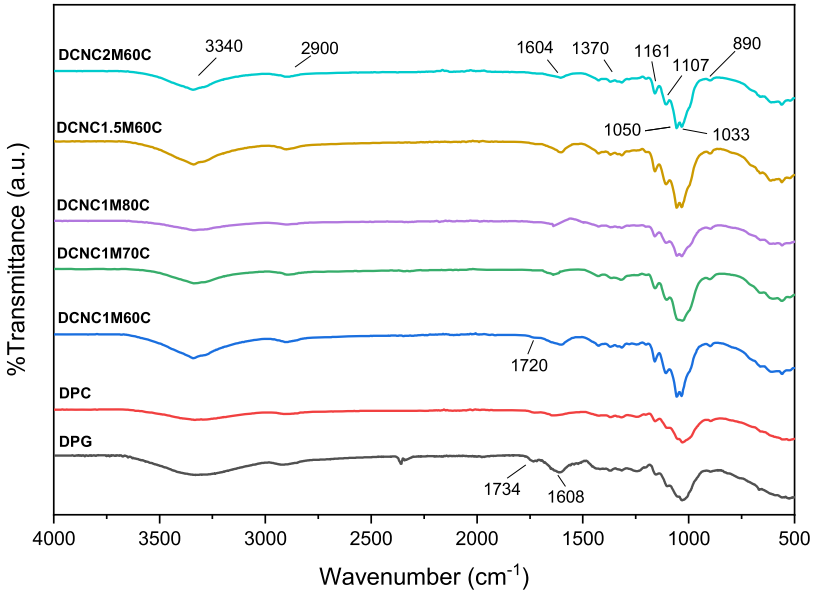

Figure 3. ATR-IR spectra of the DPG, DPC, and DCNC obtained under various oxidation temperatures and APS concentrations.

nanocrystals (DCNCs). Figure 2 demonstrates the isolation of the CNC using the APS oxidation process, and Table 1 summarizes the oxidation parameters and yields of resulting CNCs.

2.4. Characterization. *2.4.1. Yield of Cellulose Nanocrystals (CNCs).* The obtained CNC yield was measured using a gravimetric method proposed by a previous study.[27] In this method, the total volume of the resulting CNC suspension was measured (V_1), and then some CNC suspensions (V_2) were transferred to a weighing bottle (m_2), and a freeze-drying process was carried out. The CNC resulting from freeze-drying was weighed with the bottle (total mass m_1), and then the yield was obtained using eq 1

$$\text{yield} = \frac{(m_1 - m_2) \times V_1}{m_3 \times V_2 \times 52.7\%} \quad (1)$$

where m_3 is the mass of raw material and and 52.7% is the cellulose content in untreated durian peel powder.

2.4.2. Attenuated Total Reflection-Infrared (ATR-IR) Spectroscopy Analysis. ATR-IR (Shimadzu) spectroscopy was utilized to identify the chemical structure or composition, hydrogen bonds, functional groups, aromatic compounds, and phenolic compounds of lignocellulosic materials.[28] DPG, DPC, and DCNC samples were positioned directly on the ATR crystal. To make sure the samples were compact and even, the clamp was rotated until its boundary limit. A scanning resolution of 4 cm^{-1} with transmittance mode using 46 acquisitions was recorded in the range of 500 to 4000 cm^{-1} wavenumber. ATR-IR was also used to calculate the degree of oxidation (DO) of the resulting CNC using eq 2.

$$\text{DO} = 0.01 + 0.7\left(\frac{I_{1604}}{I_{1033}}\right) \quad (2)$$

where I_{1604} is the intensity of the sodium carboxylic group, and I_{1033} is the intensity of the highest peak of cellulose.[21]

2.4.3. X-ray Diffraction (XRD) Analysis. The crystalline structures of DPG, DPCs, and DCNCs were characterized by using an X-ray diffractometer (Malvern PANalytical, The Netherlands). The characterization was performed using Cu−Kα radiation (λ = 0.154 nm) in the range of 2θ = 10−50°. The speed used was 0.1°/min operating at 40 kV and 30 mA. The Segal empirical method[29] was used to examine the crystallinity index as listed in eq 3

$$\text{Cr}I = \frac{(I_{200} - I_{\text{am}})}{I_{200}} \times 100\% \quad (3)$$

where I_{200} is the maximum intensity of the (200) lattice diffraction (crystalline region) at 2θ = 22−23° and I_{am} denotes the amorphous region with the diffraction intensity at 2θ = 18−19°.

2.4.4. Thermogravimetric Analysis (TGA). To evaluate the thermal resistance of DPG, DPCs, and DCNCs, thermogravimetric analysis (Netzsch STA 449F3, Germany) was used by recording TG and DTG curves. The sample in solid form (about 20−22 mg) was put inside a crucible and heated from ambient temperature to 600 °C. The constant heating rate of

https://doi.org/10.1021/acsomega.3c03117
ACS Omega 2023, 8, 30262−30272

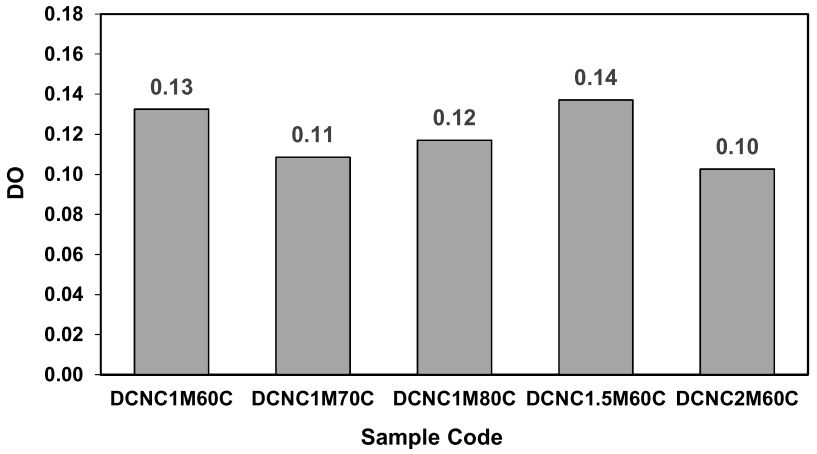

Figure 4. DO of the obtained CNC.

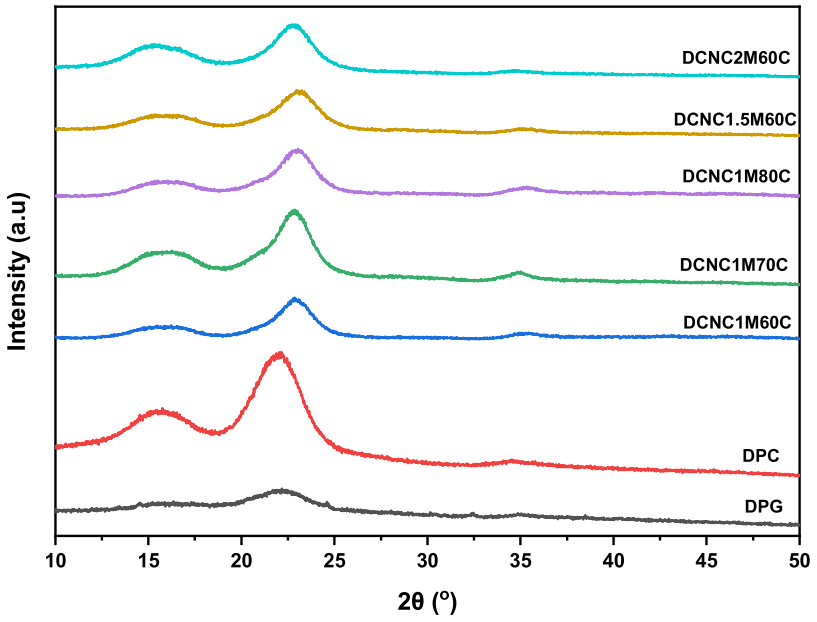

Figure 5. XRD patterns of the DPG, DPC, and obtained CNC under various oxidation parameters.

10°/min was used to evaluate the thermal degradation of the raw material and resulting CNCs. This characterization was performed under a nitrogen atmosphere.

2.4.5. Transmission Electron Microscopy (TEM) Analysis. TEM (JEOL type JEM-1400 electron microscope, Japan) was used to evaluate the morphology and dimensions of CNCs isolated from durian peel powder. The CNC supernatant was homogenized using ultrasonication for 5 min for better dispersion. A carbon-coated copper grid was dripped with the CNC supernatant and dried at room temperature. To increase the contrast of the TEM images, we dripped uranyl acetate solution onto the grid. Based on the acquired TEM images, the CNC length and width were calculated by using ImageJ software. The aspect ratio was then calculated by dividing the length and width of the TEM measurement.

3. RESULTS AND DISCUSSION

3.1. CNC Yield Measurement. The CNC produced from the isolation of durian peel powder with different oxidation parameters is shown in Table 1. The reaction parameters investigated in this study, which are the reaction temperature and APS concentration, greatly influenced the yield of CNCs. Based on the results obtained from eq 1, it can be shown that at 1 M APS concentration, the CNC yield increased with rising reaction temperature, with the sample DCNC1M80C obtaining the highest yield (35.67%). The increase in temperature resulted in more dissolution of the amorphous region, causing more extraction of the nanocellulose.

If observed further at a constant reaction temperature of 60 °C, the addition of the APS concentration decreased the yield of CNCs. The CNC yield dropped from 30.11 to 24.79% when the APS concentration was increased from 1 to 1.5 M. When the APS concentration was raised to 2 M, this continued to fall, reaching 17.65%. The high APS concentration caused a stronger oxidative reaction leading to the hydrolysis of amorphous and crystalline regions resulting in a decrease in the diameter of the cellulose.[21,30]

3.2. ATR-IR Spectroscopy Analysis. Figure 3 displays the infrared spectra of the DPG, DPC, and produced DCNC at various oxidation temperatures and APS concentrations. The peaks at 1734 and 1608 cm^{-1} found in the untreated durian peel ground (DPG) correspond to the existence of acetyl and

https://doi.org/10.1021/acsomega.3c03117
ACS Omega 2023, 8, 30262−30272

uronic ester groups of hemicellulose and aromatic vibrations of lignin, respectively.[14,31] The shortage of these two peaks in the DPC and DCNC affirms the efficient removal of lignin and hemicellulose from DPG powder after the bleaching pretreatment and APS oxidation. The peaks at 3340 and 2900 cm^{-1} indicated the O−H stretching vibration and C−H stretching vibration in cellulose molecules, respectively.[32,33]

All DCNC samples exhibited a peak of the C═O stretching vibration at 1720 cm^{-1}, indicating the carboxylic group, which is a typical characteristic of CNCs prepared using APS oxidation. Further, the broad peak at 1600 cm^{-1} observed in DCNC samples is associated with the presence of sodium carboxylate due to the neutralization of CNCs using NaOH.[17] All cellulosic samples showed absorbance bands in the spectra at 1370 and 890 cm^{-1} attributed, respectively, to the stretching vibration of cyclic C═O and β-glycosidic bonds between glucose units in cellulose.[34,35] The C−O−C pyranose ring skeletal vibration was also found by the absorption band at ∼1033 cm^{-1}.[21] The DCNC showed more intense cellulose peaks at ∼1161, 1107, and 1050 cm^{-1}. Sodium carboxylate (−COO−Na^+) groups also appeared in the spectra at ∼1604 cm^{-1}. The sharp peak attributed to the vibrations of cellulose denotes the high purity of the CNC after the combination process. There was no significant change in the IR spectra between the DPG and resulting CNC, suggesting non-destruction of the main cellulosic structures.

The degree of oxidation in this study was determined using IR spectra and is summarized in Figure 4. An increase in the intensity of the carboxyl group with an increase in the optimal concentration of APS at 1.5 M caused an increase in the degree of oxidation in the CNC. This was a result of the intense oxidation process, producing more sulfate free radicals (SO_4^-). In addition, there was more oxidation of the primary C6 hydroxyl group, which converted to a carboxyl group, and the hydrolysis of the amorphous phase of the cellulose, which was responsible for the increased degree of oxidation.[30]

3.3. XRD Analysis. The XRD patterns of the DPG, DPC, and the resulting DCNC with various oxidation temperatures and APS concentrations are summarized in Figure 5. For DPG samples, the crystalline peaks at 2θ = 16.36, 22.17, and 34.85° correspond to the (110), (200), and (004) planes of the typical structure of cellulose Iβ.[36] After the bleaching process, the peaks were shifted to 15.76, 22.14, and 34.54°. Samples chemically treated using APS (DCNC1M80C) showed almost the same peaks where these peaks related to the primary cellulose crystalline domain, with a broad peak of about 16.85° corresponding to the plane 110, a peak at 23.10° corresponding to the plane 200, and a peak at 35.22° corresponding to the plane 004. Although the cellulose has been surface-treated by bleaching pretreatment and APS oxidation, the crystalline structure of cellulose Iβ was still maintained, evidenced by the existence of those crystalline peaks as depicted in Figure 5. If the intensity of 2θ = ∼ 22° was compared between the DPG and DCNC, it could be seen that there was a remarkable improvement after oxidation, suggesting the enhancement in cellulose purity and crystallinity. Table 2 exhibits the crystallinity index of the DPG, DPC, and resulting CNC.

The crystallinity index of the DPC sample (61.90%) was higher than that of the untreated DPG sample (40.06%). This was associated with the removal of lignin and hemicellulose in amorphous areas during the bleaching pretreatment process.[33] After APS oxidation treatments, the crystallinity of all of the resulting CNCs was remarkably improved. Based on Table 2, it can be inferred that the crystal index increases with increasing oxidation temperature, with the CNC oxidized at 80 °C and 1 M APS concentration producing the highest crystal index. Compared to the untreated durian peel ground, this CNC significantly increased the crystallinity index from 40.06 to 81.62%. This was attributed to the fact that APS oxidation could cause high decomposition of amorphous cellulose areas during the process.[17] This phenomenon was in line with the results from other studies.[7,19,20] However, the addition of the APS concentration in this study led to a decrease in the CNC crystallinity index. This might be due to damage to the cellulose crystal structure with the addition of APS concentration.[21]

Table 2. Crystallinity Index of the DPG, DPC, and Obtained CNC

samples	crystallinity index (%)
DPG	40.06
DPC	61.90
DCNC1M60C	79.77
DCNC1M70C	80.82
DCNC1M80C	81.62
DCNC1.5M60C	76.47
DCNC2M60C	70.52

The CNC crystallinity index produced from durian peel waste (81.62%) in this investigation was higher when compared to most other studies using the same method, such as nanocellulose extracted from palm frond oil (52.4%),[20] balsa fiber (57.65%),[19] kapok fiber (60.71%),[19] recycled medium density fiberboard (62.7%),[21] *Pennisetum Purpureum* (66.56%),[7] *M. x. giganteus* (70%),[22] lemon seed waste (74.40%),[15] and sugar cane bagasse pulp (76.5%)[16] and lower than the industrial hybrid poplar residue (87.1%)[13] and the cotton liner (93.5%).[37] However, although the CNC crystallinity index of durian peels was lower than these two observations, the significant increase in the crystallinity index of this study was the highest compared to those of other studies in producing nanocellulose.

3.4. Thermogravimetric Analysis. As a strengthening material, the thermal stability of CNCs is particularly important for achieving minimal thermal acceptance in the manufacturing of composite materials. In general, biocomposites are processed at a temperature between 150 and 300 °C, depending on the type of matrix used. In composite processing, the minimum temperature required is around 180−200 °C.[38] Figure 6 summarizes the results of the thermogravimetric characterization in the form of TG and DTG curves from the obtained DPG, DPC, and DCNC, while the initial degradation temperature, maximum degradation temperature, and charcoal residue are presented in Table 3. As demonstrated in Figure 6a, the evaporation of the water content was indicated by a reduction of 10% in the weight of the sample at temperatures below 100 °C.[33,39] Large mass loss was shown for all samples at 200−340 °C, indicating that there was pyrolysis of cellulose.[40] Further, there was also weight loss at the temperature range of 340−600 °C, which corresponded to the advanced breaking of glycosidic bonds. In addition, at this temperature interval, the deterioration of the carbon-containing skeleton with the employment of the production of the charred residue and low molecular weight compounds was also developed.[41]

https://doi.org/10.1021/acsomega.3c03117
ACS Omega 2023, 8, 30262−30272

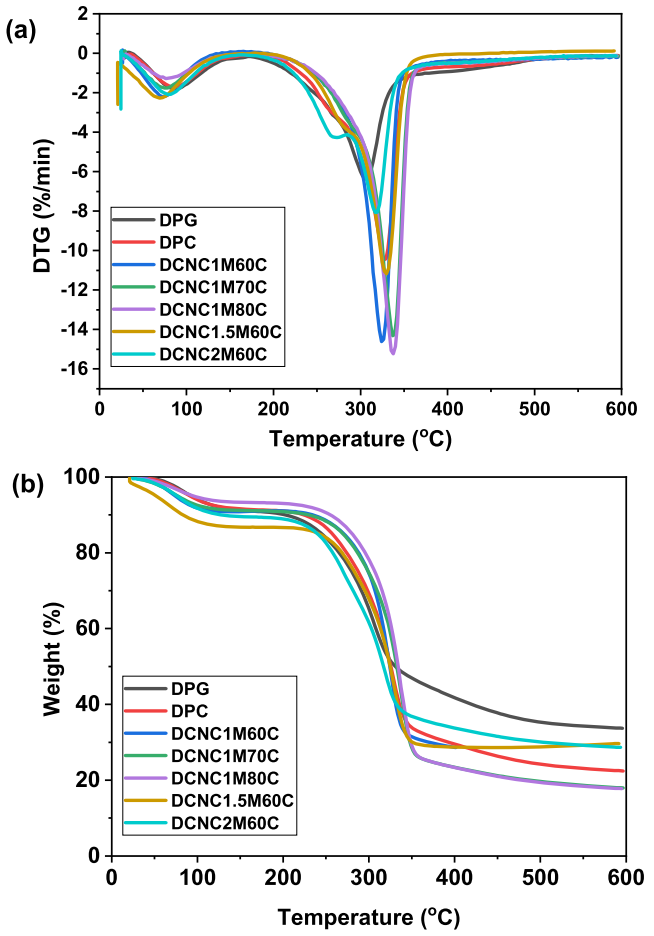

Figure 6. TG (a) and DTG (b) curves of the DPG, DPC, and obtained CNC.

Table 3. Initial Degradation Temperatures, Maximum Degradation Temperatures, and the Char Residue Yield of the DPG, DPC, and the Obtained CNC

samples	initial degradation temperature (°C)	maximum degradation temperature (°C)	char residue yield (%)
DPG	263.6	307.17	33.69
DPC	287.0	326.46	22.44
DCNC1M60C	296.2	324.59	23.05
DCNC1M70C	304.5	336.96	17.94
DCNC1M80C	306.5	337.67	17.77
DCNC1.5M60C	291.7	329.79	29.68
DCNC2M60C	269.0	316.97	28.64

It could be summarized from Table 3 that the early stage of degradation and maximum degradation temperatures of all CNCs were higher than the untreated one suggesting better thermal stability of CNCs. The results of the TGA test also revealed that an increase in the oxidation temperature resulted in better thermal stability of the material, where the CNC with the highest initial degradation temperature (306.5 °C) and maximum degradation temperature (337.67 °C) belonged to the DCNC1M80C sample. This was supported by the XRD result, where the highest crystal index was achieved by that CNC. Thus, it could be said that at 80°C and 1 M APS, the process of dissolving amorphous regions was more effective than that at other temperatures and concentrations. These findings were inconsistent with previous results where most initial and maximum degradation temperatures decreased after the raw material was isolated.[15,16] This was possibly associated with differences in the raw cellulose characteristics, oxidation parameters, and experimental procedures. However, compared to the raw materials, all of the CNCs obtained in this work exhibited a much higher heat resistance.

Furthermore, the thermal stability of the CNC was decreased by the increase in APS concentration, where the initial degradation temperature of DCNC2M60C (269.0 °C) was lower than those of DCNC1M60C (296.2 °C) and DCNC1.5M60C (291.7 °C). Partial damage to the cellulose structure and a wider surface area exposed to heat may be the cause of the low initial degradation temperature of the DCNC2M60C sample. These results were in line with other studies where higher APS concentrations can allow for a decrease in the initial degradation temperature of a material.[20]

It is clear from the char residue that an increase in the oxidation temperature results in a reduction in yield. The final char residue at 600 °C of the DCNC with a 1 M APS concentration was 23.05% for CNCs oxidized at 60°C, 17.94% for CNCs oxidized at 70°C, and 17.77% for CNCs oxidized at 80°C. The char residues of DCNC1M70C and DCNC1M80C were significantly lower than that of the untreated durian peel ground (33.69%). This phenomenon was probably due to the high lignin content of durian peel, which decomposes over a broad range of temperatures (150−900 °C).[42] In addition, the char residue of the CNC processed with 1 M APS (23.05%) was lower than those of CNCs processed with 1.5 M (29.68%) and 2 M (28.64%). This is possibly due to the higher APS concentration requiring higher sodium hydroxide to neutralize the acidity of the CNC suspension. The sodium carboxylate group on the CNC surface acted as a flame retardant, meaning that the higher the concentration of APS, the higher the probability of the residue being produced.[18]

In addition, from the DTG curve (Figure 6b), it can be seen that for the decomposition rate, DPG (307.17 °C) is the sample with the lowest temperature, which achieved the maximum decomposition. This indicated that the sample has the least good thermal stability due to its low CrI (40.06%). In comparison, the DPC and DCNC samples showed a higher maximum decomposition temperature, where the value almost reached 340 °C, indicating the occurrence of cellulose decomposition.[43] In general, it can be said that the good thermal stability of CNCs was contributed by the high degree of purity of cellulose and the effective removal of amorphous regions.[44,45]

3.5. Transmission Electron Microscopy Aanalysis. The dimensions and morphology of the resulting CNC were evaluated by using TEM. Figure 7 represents the TEM images of CNCs isolated from durian peel waste at different oxidation temperatures and at different magnifications. It can be seen that all CNCs show a needlelike structure with nanosize, indicating the successful preparation of CNCs. Based on the figure, it is clear that the nanocellulose content in the DCNC1M70C (Figures 7d−f) and DCNC1M80C (Figures 7g−i) supernatants was more than that of DCNC1M60C (Figures 7a−c). This may be due to less reduction in amorphous areas due to oxidation occurring at lower temperatures, resulting in larger particles in the CNC suspension. When the suspension was centrifuged, large cellulose gathers at the bottom to become a precipitate and was removed from the suspension. This resulted in a higher

https://doi.org/10.1021/acsomega.3c03117
ACS Omega 2023, 8, 30262−30272

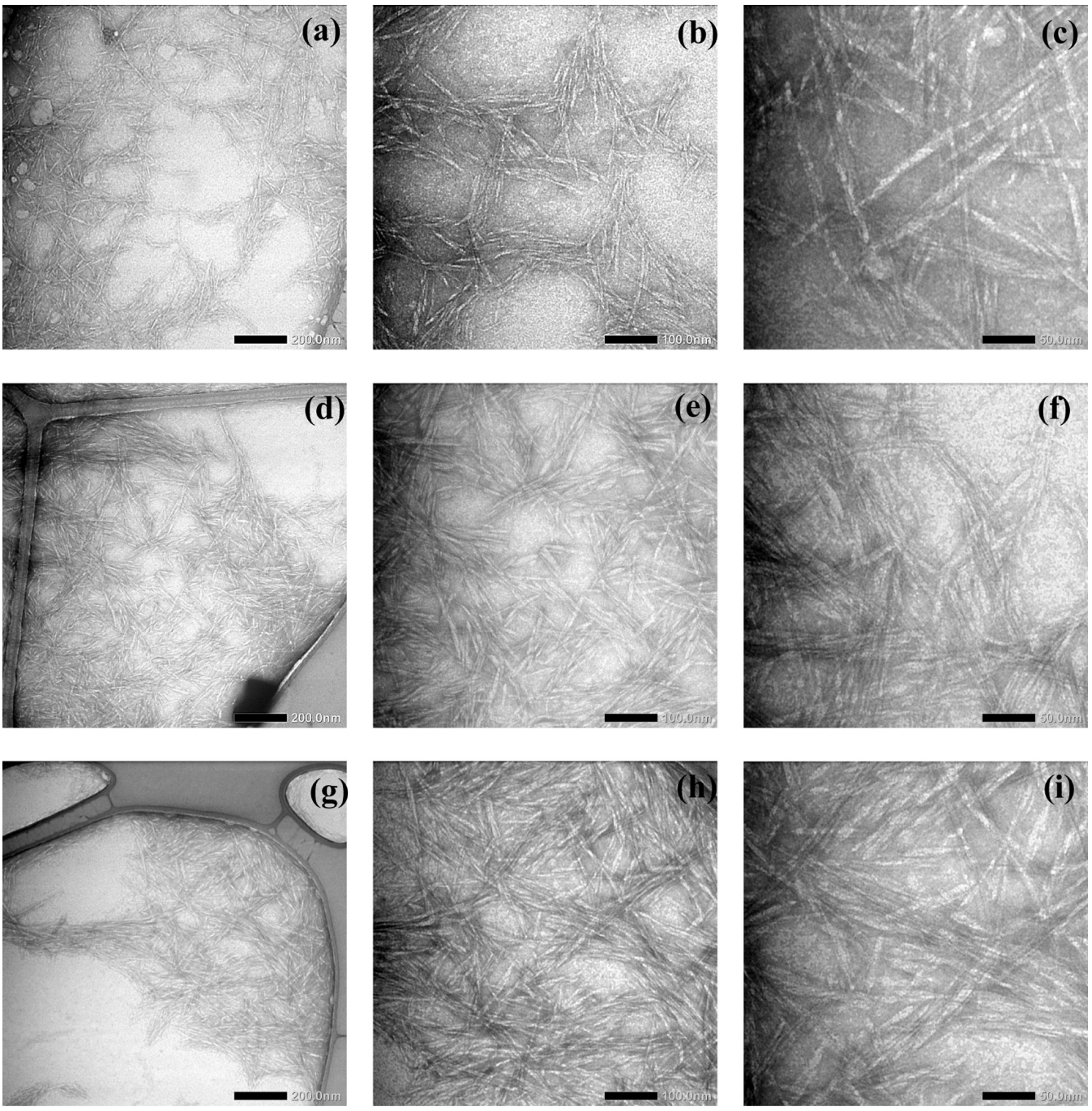

Figure 7. TEM images of resulting CNCs with different magnifications under various oxidation temperatures: (a−c) 60 °C, (d−f) 70 °C, and (g−i) 80 °C.

CNC content found in the supernatant at a reaction temperature of 80°C compared to the reaction temperature of 60°C.

The distribution of the width and length of the CNC measured from the TEM images and the aspect ratio based on the width and length are shown in Figure 8. The results showed that the average values of 1 M APS concentration samples prepared for 16 h at different reaction temperatures ranged from 5.00 to 7.81 nm for the width and from 114.52 to 126.83 nm for the length. It can be observed that the dimensions of the CNC prepared at 60 °C have a length of 95−149 nm and a width of 4.7−10.5 nm. However, the CNC treated at a higher temperature has a smaller diameter and a slightly shorter length. When the process temperature is increased to 80 °C, CNCs with a length of 140−500 nm and a diameter of 3.1−7.9 nm are obtained. This might be because the higher oxidation temperature was able to remove amorphous regions such as layers of wax, hemicellulose, and lignin more than the lower temperature, resulting in a relatively smaller diameter.

The width of the CNC in this study was smaller compared to other studies that also used APS as a nanocellulose-producing agent. Zhang et al. reported that the CNC sourced from bleached sugar cane bagasse pulp has a width of 20 to 109 nm, while the CNC produced from MDF fibers has a width of 13 to 17 nm, and CNCs isolated from lemon seeds

https://doi.org/10.1021/acsomega.3c03117
ACS Omega 2023, 8, 30262−30272

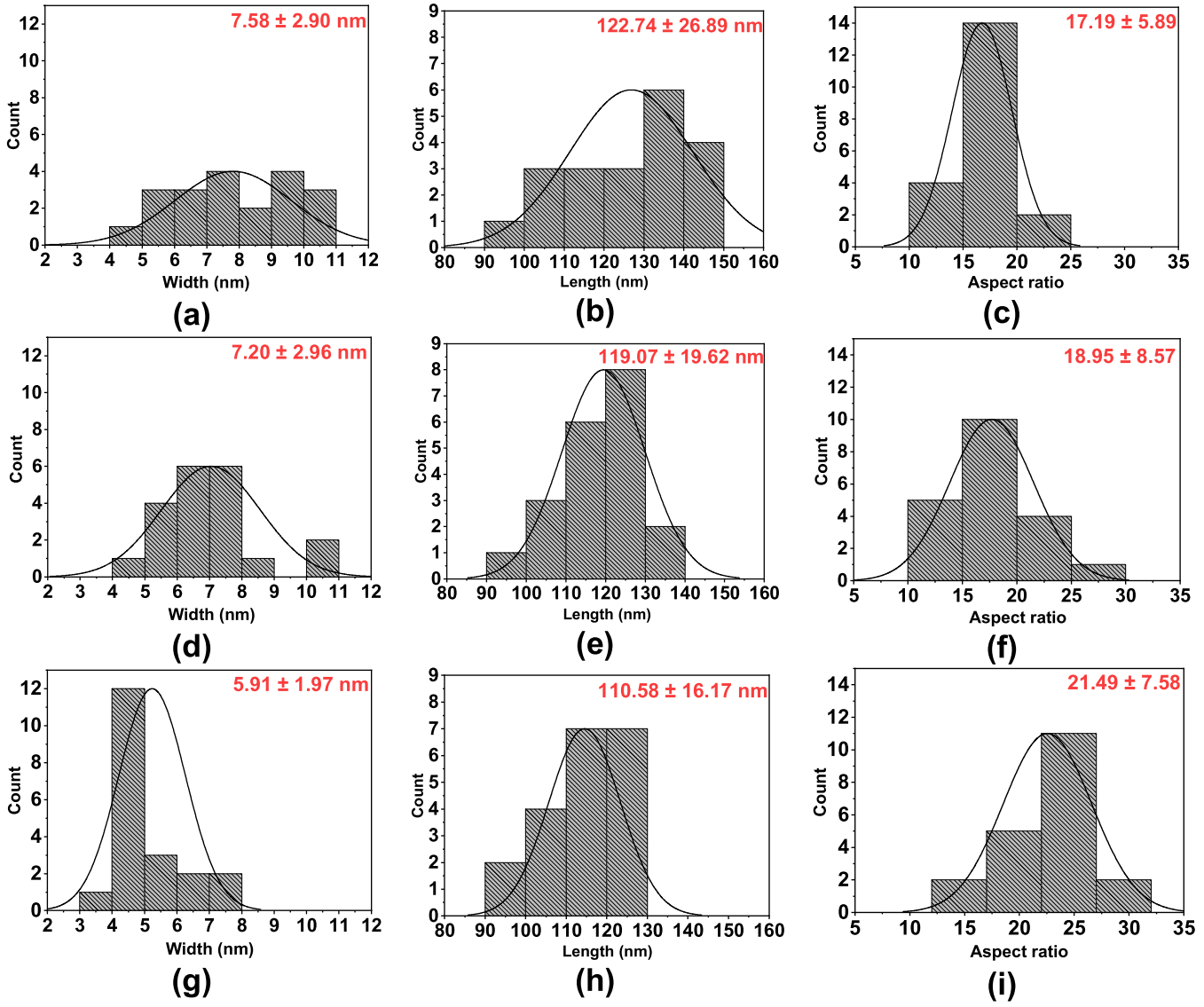

Figure 8. Width, length, and aspect ratio of resulting CNCs: (a–c) DCNC1M60C; (d–f) DCNC1M70C; and (g–i) DCNC1M80C.

have a width of 10 to 20 nm.[15,16,21] However, the CNC produced from this investigation was shorter than that from the above studies. This was attributed to several things such as raw materials, isolation methods, and several other experimental factors. In contrast, an investigation has shown that the length of the nanocellulose has almost no effect on the water vapor barrier properties when utilized in the composite.[46]

Unlike the width and length, the aspect ratio of nanocellulose increases with an increasing reaction temperature, as shown in Figure 8c,f,i. This is due to a significant reduction in the width and a slight reduction in the length due to depolymerization. The highest value was obtained by DCNC1M80C with an aspect ratio of 26.11 ± 12.19, and the lowest was obtained by DCNC1M60C with an aspect ratio of 17.19 ± 5.89. The aspect ratio of the obtained CNC was considerably high compared to that from the investigation done by Jiang et al. and Khanjanzadeh and Park.[13,21] Thus, the dimensions of the nanocellulose measured by TEM images are consistent with the results of other tests, such as the degree of oxidation, XRD, and TGA to a certain extent.

4. CONCLUSIONS

Regardless of the oxidation temperature and APS concentration, the CNC structure obtained from durian rind waste was still consistent with that of raw cellulose. The APS concentration and oxidation temperature greatly affect the characteristics of the CNC produced. A much higher crystallinity index and thermal stability were demonstrated by the resulting CNC compared to the untreated durian peel ground. XRD results indicated that the crystallinity index of the CNC improved as the oxidation temperature increased. The highest index was reached when the sample was surface-treated with APS at 1 M and 80 °C, resulting in nanocellulose with a crystallinity of 81.62% from the untreated one with a crystallinity of 40.06%. The CNC isolated with 1 M APS at 80 °C had the highest initial degradation temperature of 306.5 °C and the maximum degradation temperature of 337.67 °C. However, the addition of APS concentration caused a significant decrease in the crystallinity index and thermal resistance. Morphology results concealed the fact that the increase in the oxidation temperature and the addition of APS concentration contributed to the reduction in the CNC width

https://doi.org/10.1021/acsomega.3c03117
ACS Omega 2023, 8, 30262−30272

and length. Several investigations in recent years have investigated methods for isolating CNCs; however, these processes are toxic, nonrenewable, and consume high levels of energy. APS oxidation is probably the best approach to increase the waste value without adversely impacting the environment; regardless, future studies should address the issue of improving the yield and aspect ratio through some experimental modifications. Overall, the obtained CNC from durian peel waste had great potential for reinforcing the material of bionanocomposites.

AUTHOR INFORMATION

Corresponding Author

Kusmono − *Department of Mechanical and Industrial Engineering, Faculty of Engineering, Universitas Gadjah Mada, Yogyakarta 55281, Indonesia;* orcid.org/0000-0003-1465-3013; Email: kusmono@ugm.ac.id

Authors

Henny Pratiwi − *Department of Mechanical and Industrial Engineering, Faculty of Engineering, Universitas Gadjah Mada, Yogyakarta 55281, Indonesia; Department of Mechanical Engineering Education, Faculty of Engineering, Universitas Negeri Yogyakarta, Yogyakarta 55281, Indonesia*

Muhammad Waziz Wildan − *Department of Mechanical and Industrial Engineering, Faculty of Engineering, Universitas Gadjah Mada, Yogyakarta 55281, Indonesia*

Complete contact information is available at: https://pubs.acs.org/10.1021/acsomega.3c03117

Notes

The authors declare no competing financial interest.

ACKNOWLEDGMENTS

Financial support provided by the Center for Higher Education Funding (BPPT) and Indonesia Endowment Fund for Education (LPDP) on decree no. 1410/J5.2.3./BPI.06/10/2021 is greatly appreciated.

REFERENCES

(1) Sharma, A.; Thakur, M.; Bhattacharya, M.; Mandal, T.; Goswami, S. Commercial application of cellulose nano-composites − A review. *Biotechnol. Rep.* **2019**, *21* (2018), No. e00316.

(2) Qin, Y.; Mo, J.; Liu, Y.; et al. Stretchable Triboelectric Self-Powered Sweat Sensor Fabricated from Self-Healing Nanocellulose Hydrogels. *Adv. Funct. Mater.* **2022**, *32* (27), No. 2201846.

(3) Gao, C.; Liu, T.; Luo, B.; et al. Cellulosic triboelectric materials for stable energy harvesting from hot and humid conditions. *Nano Energy* **2023**, *111*, No. 108426.

(4) Shao, Y.; Luo, B.; Liu, T.; et al. Harvesting energy from extreme environmental conditions with cellulosic triboelectric materials. *Mater. Today* **2023**, *66*, 348−370.

(5) Lavanya, D.; Kulkarni, P. K.; Dixit, M.; Raavi, P. K.; Krishna, L. N. V. Sources of cellulose and their applications- A review. *Int. J. Drug Formulation Res.* **2015**, *2*, 19−38.

(6) Ferrer, A.; Pal, L.; Hubbe, M. A. Nanocellulose in packaging: Advances in barrier layer technologies. *Ind. Crops Prod.* **2017**, *95*, 574−582.

(7) Aryasena, R.; Kusmono; Umami, N. Production of cellulose nanocrystals extracted from Pennisetum purpureum fibers and its application as a lubricating additive in engine oil. *Heliyon* **2022**, *8* (11), No. e11315.

(8) Kusmono; Listyanda, R. F.; Wildan, M. W.; Ilman, M. N. Preparation and characterization of cellulose nanocrystal extracted from ramie fibers by sulfuric acid hydrolysis. *Heliyon* **2020**, *6* (11), No. e05486.

(9) Jafarzadeh, S.; Jafari, S. M.; Salehabadi, A.; Nafchi, A. M.; Kumar, U. S. U.; Khalil, H. P. S. A. Biodegradable green packaging with antimicrobial functions based on the bioactive compounds from tropical plants and their by-products. *Trends Food Sci. Technol.* **2020**, *100*, 262−277.

(10) Li, M.; He, B.; Chen, Y.; Zhao, L. Physicochemical Properties of Nanocellulose Isolated from Cotton Stalk Waste. *ACS Omega* **2021**, *6* (39), 25162−25169.

(11) Wijaya, C. J.; Ismadji, S.; Aparamarta, H. W.; Gunawan, S. Hydrophobic modification of cellulose nanocrystals from bamboo shoots using rarasaponins. *ACS Omega* **2020**, *5* (33), 20967−20975.

(12) Imanzadeh, G. H.; Zamanloo, M. R.; Mansoori, Y.; Khodayari, A. Aqueous Media Oxidation of Alcohols with Ammonium Persulfate. *Chin. J. Chem.* **2007**, *25* (6), 836−838.

(13) Jiang, H.; Wu, Y.; Han, B.; Zhang, Y. Effect of oxidation time on the properties of cellulose nanocrystals from hybrid poplar residues using the ammonium persulfate. *Carbohydr. Polym.* **2017**, *174*, 291−298.

(14) Hu, Y.; Tang, L.; Lu, Q.; Wang, S.; Chen, X.; Huang, B. Preparation of cellulose nanocrystals and carboxylated cellulose nanocrystals from borer powder of bamboo. *Cellulose* **2014**, *21* (3), 1611−1618.

(15) Zhang, H.; Chen, Y.; Wang, S.; et al. Extraction and comparison of cellulose nanocrystals from lemon (Citrus limon) seeds using sulfuric acid hydrolysis and oxidation methods. *Carbohydr. Polym.* **2020**, *238* (2), No. 116180.

(16) Zhang, K.; Sun, P.; Liu, H.; Shang, S.; Song, J.; Wang, D. Extraction and comparison of carboxylated cellulose nanocrystals from bleached sugarcane bagasse pulp using two different oxidation methods. *Carbohydr. Polym.* **2016**, *138*, 237−243.

(17) Leung, A. C. W.; Hrapovic, S.; Lam, E.; et al. Characteristics and Properties of Carboxylated Cellulose Nanocrystals Prepared from a Novel One-Step Procedure. *Small* **2011**, *7* (3), 302−305.

(18) Indirasetyo, N. L.; Kusmono. Isolation and Properties of Cellulose Nanocrystals Fabricated by Ammonium Persulfate Oxidation from Sansevieria trifasciata Fibers. *Fibers* **2022**, *10* (7), No. 61.

(19) Marwanto, M.; Maulana, M. I.; Febrianto, F.; et al. Effect of oxidation time on the properties of cellulose nanocrystals prepared from balsa and kapok fibers using ammonium persulfate. *Polymers* **2021**, *13* (11), No. 1894.

(20) Zaini, L. H.; Febrianto, F.; Wistara, I. N. J.; et al. Effect of ammonium persulfate concentration on characteristics of cellulose nanocrystals from oil palm frond. *J. Korean Wood Sci. Technol.* **2019**, *47* (5), 597−606.

(21) Khanjanzadeh, H.; Park, B. D. Optimum oxidation for direct and efficient extraction of carboxylated cellulose nanocrystals from recycled MDF fibers by ammonium persulfate. *Carbohydr. Polym.* **2021**, *251*, No. 117029.

(22) Yang, H.; Zhang, Y.; Kato, R.; Rowan, S. J. Preparation of cellulose nanofibers from *Miscanthus x. Giganteus* by ammonium persulfate oxidation. *Carbohydr. Polym.* **2019**, *212*, 30−39.

(23) Kusumaningtyas, R. D.; Suyitno, H.; Wulansarie, R. Pengolahan Limbah Kulit Durian Di Wilayah Gunungpati Menjadi Biopestisida Yang Ramah Lingkungan. *Rekayasa: J. Penerapan Teknol. Pembelajaran* **2018**, *15* (1), 38−43.

(24) Pratiwi, M.; Kawuri, R.; Ardhana, I. P. Potensi antibakteri limbah kulit durian (Durio zibethinus Murr.) terhadap Propionibacterium acnes penyebab jerawat Antibacterial potency from the waste of durian rind (Durio zibethinus Murr.) against Propionibacterium a cnes that causing acnes. *J. Biol. Udayana* **2019**, *23* (1), 8−15.

(25) Rosmawati, T. Pemanfaatan Limbah Kulit Durian Sebagai Bahan Baku Briket Dan Pestisida Nabati. *Biosel Biol. Sci. Educ.* **2016**, *5* (2), 159−170.

(26) Nur Aimi, M. N.; Anuar, H.; Maizirwan, M.; Sapuan, S. M.; Wahit, M. U.; Zakaria, S. Preparation of durian skin nanofibre

https://doi.org/10.1021/acsomega.3c03117
ACS Omega 2023, 8, 30262−30272

(DSNF) and its effect on the properties of polylactic acid (PLA) biocomposites. *Sains Malays.* **2015**, *44* (11), 1551−1559.
(27) Lu, Q.; Cai, Z.; Lin, F.; Tang, L.; et al. Extraction of Cellulose Nanocrystals with a High Yield of 88% by Simultaneous Mechanochemical Activation and Phosphotungstic Acid Hydrolysis. *ACS Sustainable Chem. Eng.* **2016**, *4*, 2165−2172.
(28) Md Salim, R.; Asik, J.; Sarjadi, M. S. Chemical functional groups of extractives, cellulose and lignin extracted from native Leucaena leucocephala bark. *Wood Sci. Technol.* **2021**, *55* (2), 295−313.
(29) Segal, L.; Creely, J. J.; Martin, A. E.; Conrad, C. M. An Empirical Method for Estimating the Degree of Crystallinity of Native Cellulose Using the X-Ray Diffractometer. *Text. Res. J.* **1959**, *29* (10), 786−794.
(30) Cheng, M.; Qin, Z.; Liu, Y.; Qin, Y.; Li, T. Efficient extraction of carboxylated spherical cellulose nanocrystals with narrow distribution through hydrolysis of lyocell fi bers by using ammonium persulfate as an oxidant. *J. Mater. Chem. A* **2014**, 251−258.
(31) He, T.; Jiang, Z.; Wu, P.; Yi, J.; Li, J.; Hu, C. Fractionation for further conversion: from raw corn stover to lactic acid. *Sci. Rep.* **2016**, *6* (1), No. 38623.
(32) Maiti, S.; Jayaramudu, J.; Das, K.; et al. Preparation and characterization of nano-cellulose with new shape from different precursor. *Carbohydr. Polym.* **2013**, *98* (1), 562−567.
(33) Dai, H.; Ou, S.; Huang, Y.; Huang, H. Utilization of pineapple peel for production of nanocellulose and film application. *Cellulose* **2018**, *25* (3), 1743−1756.
(34) Haafiz, M. K. M.; Hassan, A.; Zakaria, Z.; Inuwa, I. M. Isolation and characterization of cellulose nanowhiskers from oil palm biomass microcrystalline cellulose. *Carbohydr. Polym.* **2014**, *103*, 119−125.
(35) Dai, H.; Huang, Y.; Zhang, H.; et al. Direct fabrication of hierarchically processed pineapple peel hydrogels for efficient Congo red adsorption. *Carbohydr. Polym.* **2020**, *230*, No. 115599.
(36) Deepa, B.; Abraham, E.; Cordeiro, N.; et al. Utilization of various lignocellulosic biomass for the production of nanocellulose: a comparative study. *Cellulose* **2015**, *22* (2), 1075−1090.
(37) Oun, A. A.; Rhim, J. W. Characterization of carboxymethyl cellulose-based nanocomposite films reinforced with oxidized nano-cellulose isolated using ammonium persulfate method. *Carbohydr. Polym.* **2017**, *174*, 484−492.
(38) Mohanty, A. K.; Misra, M.; Hinrichsen, G. Biofibres, biodegradable polymers and biocomposites: An overview. *Macromol. Mater. Eng.* **2000**, *276−277* (1), 1−24.
(39) Liu, C.; Li, B.; Du, H.; et al. Properties of nanocellulose isolated from corncob residue using sulfuric acid, formic acid, oxidative and mechanical methods. *Carbohydr. Polym.* **2016**, *151*, 716−724.
(40) Niu, F.; Li, M.; Huang, Q.; et al. The characteristic and dispersion stability of nanocellulose produced by mixed acid hydrolysis and ultrasonic assistance. *Carbohydr. Polym.* **2017**, *165*, 197−204.
(41) Tian, C.; Yi, J.; Wu, Y.; Wu, Q.; Qing, Y.; Wang, L. Preparation of highly charged cellulose nanofibrils using high-pressure homogenization coupled with strong acid hydrolysis pretreatments. *Carbohydr. Polym.* **2016**, *136*, 485−492.
(42) Yang, H.; Yan, R.; Chen, H.; Zheng, C.; Lee, D. H.; Liang, D. T. In-Depth Investigation of Biomass Pyrolysis Based on Three Major Components: Hemicellulose, Cellulose and Lignin. *Energy Fuels* **2006**, *20* (1), 388−393.
(43) Goh, K. Y.; Ching, Y. C.; Chuah, C. H.; Abdullah, L. C.; Liou, N. S. Individualization of microfibrillated celluloses from oil palm empty fruit bunch: comparative studies between acid hydrolysis and ammonium persulfate oxidation. *Cellulose* **2016**, *23* (1), 379−390.
(44) Trache, D.; Hussin, M. H.; Haafiz, M. K. M.; Thakur, V. K. Recent progress in cellulose nanocrystals: sources and production. *Nanoscale* **2017**, *9* (5), 1763−1786.
(45) Yu, H.; Qin, Z.; Liang, B.; Liu, N.; Zhou, Z.; Chen, L. Facile extraction of thermally stable cellulose nanocrystals with a high yield of 93% through hydrochloric acid hydrolysis under hydrothermal conditions. *J. Mater. Chem. A* **2013**, *1* (12), 3938−3944.
(46) Fukuzumi, H.; Saito, T.; Isogai, A. Influence of TEMPO-oxidized cellulose nanofibril length on film properties. *Carbohydr. Polym.* **2012**, *93*, 172−177.

https://doi.org/10.1021/acsomega.3c03117
ACS Omega 2023, 8, 30262−30272